Article ID: 1671-3664(2006)02-0245-11

Nonlinear pushover analysis of infilled concrete frames

Chao Hsun Huang (黃昭勳)[1†] Yungting Alex Tuan (段永定)[†] and Ruo Yun Hsu (許若芸)[‡]

1. *Department of Civil Engineering, Taipei University of Technology, Chinese Taipei*
2. *Department of Construction, Tamkang University, Chinese Taipei*
3. *Tien Shiang Structural and Civil Association, Chinese Taipei*

Abstract: Six reinforced concrete frames with or without masonry infills were constructed and tested under horizontal cyclic loads. All six frames had identical details in which the transverse reinforcement in columns was provided by rectangular hoops that did not meet current ACI specifications for ductile frames. For comparison purposes, the columns in three of these frames were jacketed by carbon-fiber-reinforced-polymer (CFRP) sheets to avoid possible shear failure. A nonlinear pushover analysis, in which the force-deformation relationships of individual elements were developed based on ACI 318, FEMA 356, and Chen's model, was carried out for these frames and compared to test results. Both the failure mechanisms and impact of infills on the behaviors of these frames were examined in the study. Conclusions from the present analysis provide structural engineers with valuable information for evaluation and design of infilled concrete frame building structures.

Keywords: pushover analysis; FEMA 356; infilled concrete frames; infill masonry panels; fiber-reinforced-polymer

1 Introduction

In traditional engineering design, the safety of a building is established on the margin of its structural capacity over the code-specified design load. In such an approach, designers usually have limited knowledge on the actual behavior of structures under extreme (i.e., failure or near-failure) conditions; seldom could they determine an accurate prediction of the level of structural damage in the post-yield stage. For designs governed by gravity loads, the above issue is not a major concern; for buildings subjected to high seismic load, however, the deformability of a structure at which it gets to keep its primary function becomes highly significant since engineers often rely on the ductility of structures to reduce the design seismic load.

Research on the nonlinear behavior of concrete buildings has been carried out in the past several decades. Early studies on the force-deformation relationships of concrete structures were conducted by Giberson (1967), Takeda *et al*. (1970), Otani and Sozen (1972), and Saiidi and Sozen (1979), as well as other researchers. Analytical methods developed based on these studies were widely concrete structures. However, most of these methods were too complicated to be used in actual building design, and, therefore, their application in the early years was mainly academic. In 1973, a well-known computer program for nonlinear analysis of structures, DRAN-2D, was introduced by Kanaan and Powell (1973). Since then, a number of engineering programs for nonlinear analysis of building structures, such as ANSR (Oughourlian and Powell, 1982), IDARC (Park *et al*., 1987), SARCF (Chung *et al*., 1988), and DRAIN-2DX (Allahabadi and Powell, 1988) have been introduced. In order to incorporate nonlinear elements in the design of buildings, commercial software such as ETABS (Habibullah, 1995) and SAP (Wilson, 1995) were also revised to provide nonlinear functions. As the development of computer hardware and software continued, nonlinear analysis became achievable for structural engineers. Therefore, the Structural Engineers Association of California (SEAOC) decided to include nonlinear (pushover) analysis as part of its proposed procedure for the seismic evaluation of structures, commonly referred to as performance-based design, in its Vision 2000 Report (SEAOC, 1995). Such a procedure was soon adopted in subsequent design guidelines such as ATC-40 (1996), FEMA 273 (1997), and FEMA 356 (2000), and it is now being used worldwide.

In performance-based design, the seismic performance of a building is analyzed at various levels of deformation (or seismic hazards). Then, the structural system is designed to meet the demands of individual owners based on pre-estimated construction cost. Since nonlinear analysis is required in this

Correspondence to: Chao Hsun Huang, Department of Civil Engineering, Taipei University of Technology, No. 1, Section 3, Chung Hsiao East Road, Chinese Taipei
Tel: 886-2-2771-2171 ext 2657; Fax: 886-2-2781-4518
E-mail: steve@ntut.edu.tw
[†]Associate Professor; [‡]Structural Engineer

Supported by: Science Council of Chinese Taipei Under Grant No. SC-92-2625-Z-027-003
Received December 23, 2005; **Accepted** February 22, 2006

approach, engineers have to define the load-deformation relationship for each structural component in the structural system. The Prestandard and Commentary for the Seismic Rehabilitation of Buildings published by Federal Emergency Management Agency (FEMA, 2000), also known as FEMA 356, now provides basic guidelines on the definition of post-yield behavior for various structural elements. For the strength calculation of concrete elements specifically, information can be found in the Building Code Requirements for Structural Concrete and Commentary, published by the American Concrete Institute (ACI 318, 1999). And, for strength calculation and modeling of unreinforced masonry infills, recommendations were given by researchers such as Paulay and Priestley (1992).

During the 1999 Chi-Chi Earthquake, many low-rise concrete buildings in Taiwan suffered serious damage or even collapsed. As extensive investigation conducted on these buildings (Tsai *et al*., 2000), showed that two major problems were commonly observed. The first was the poor (non-ductile) detailing of framing members, which was characterized by both the lack of transverse reinforcement and ineffective hoop anchorage (with 90° hooks) in the column area, a typical feature in buildings constructed prior to the early 1980's. The second was the presence of infill panels, especially the perforated ones, considerably altered the strong-column-weak-beam mechanism originally conceived by the designers. In order to study the failure mechanisms of these (non-ductile) structures and verify a proposed retrofit method, an experimental investigation was performed by Huang *et al*. (2006) at the Center for Research on Earthquake Engineering in Chinese Taipei. In this study, six concrete frame units were constructed with features commonly found in earthquake-damaged structures, i.e., inadequate transverse reinforcement in the column areas. To study the influence of masonry infills on the behavior of concrete frames, these specimens were constructed with either full, perforated, or no infill panels. To reproduce the damage pattern of the targeted structures (i.e., buildings damaged during the Chi-Chi Earthquake), the beams in the frames were made stronger than the columns to ensure that the failure would take place in the columns. And to verify the effectiveness of the proposed retrofit method, the columns in three of the specimens were jacketed with carbon-fiber-reinforced-polymer (CFRP) sheets to increase the shear strength of the columns, as shown in Fig. 1.

The analysis presented in this paper was to verify the applicability of the structural model developed based on the strength formulas given in ACI 318, the hinge parameters provided in FEMA 356, and the masonry force-deformation model proposed by Chen. Findings in this research should be able to help engineers improve their knowledge on the applicability of current design guidelines as well as the nonlinear behavior of concrete structures during an earthquake.

2 Description of specimens

Six concrete frames of identical dimensions and reinforcement details were constructed and tested under simulated seismic loading, as shown in Fig. 1. All six units were 220 cm in height, measured from the column base to the top of the beam, and the span length between the centerlines of the columns was 300 cm. Both the beams and columns in each frame had a cross section of 30 cm × 50 cm, as shown in Fig. 2. To ensure that the primary damage would occur in the columns, the column confinement was provided by rectangular hoops spaced at 30 cm on centers with 90° hooks at both ends, as observed in many nonductile concrete structures, and the beams were designed with a flexural strength greater than the columns with the transverse reinforcement conforming to the seismic provisions in ACI 318. With the interest of research being shear and flexural mechanisms, slipping of longitudinal bars due to lap splices was prohibited by keeping all longitudinal reinforcement continuous throughout the entire length of the columns. To represent different frame configurations, full or partial brick panels (f'_m = 6.2 MPa) of 22 cm in thickness were constructed in four of the six units, in which units with full, partial, or no infill were designated as BMNF10B, BMNFH10B, or BMNF, respectively. For

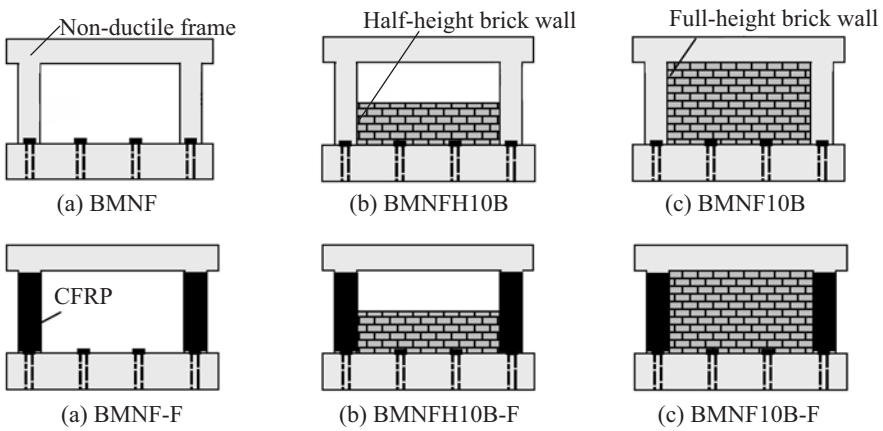

Fig. 1 Test units

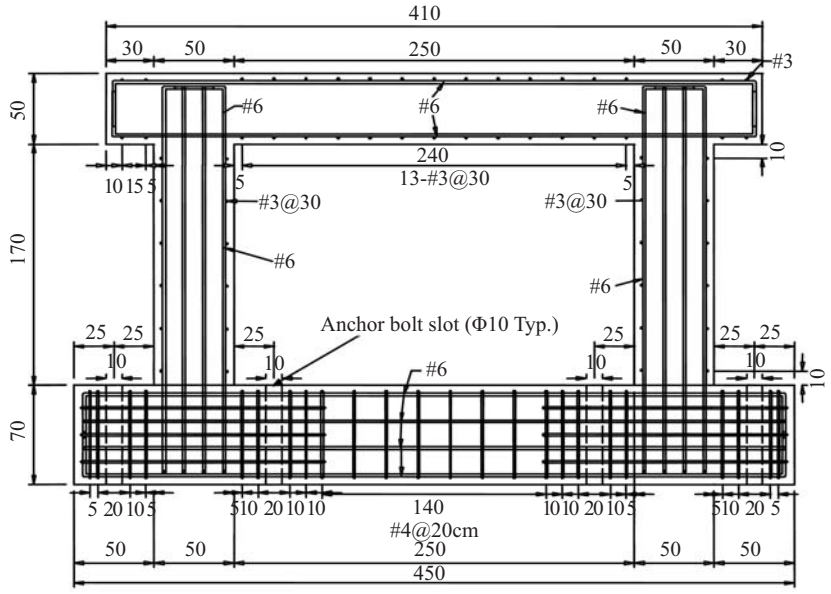

Fig. 2 Frame details (in cm)

Table 1 Frame characteristics

Unit ID	Panel height	Retrofit	Failure mechanism	Panel behavior
BMNF	N.A.	No	Column shear failure	N.A.
BMNFH10B	85 cm	No	Column shear failure	Sliding along bed joints
BMNF10B	170 cm	No	Column shear failure	Sliding along bed joints
BMNF-F	N.A.	CFRP	Column flexural failure	N.A.
BMNFH10B-F	85 cm	CFRP	Column flexural failure	Sliding along bed joints
BMNF10B-F	170 cm	CFRP	Column flexural failure	Sliding along bed joints

each of the above configurations, one of the specimens was jacketed with CFRP sheets in the column area, as indicated by the extension 'F' in the unit ID's (see Fig. 1 and Table 1).

Ready-mix normal weight concrete with an average compressive strength of 19.5 MPa was used in all frame units. Longitudinal reinforcement in all framing members was provided by #6, grade 60 bars ($f_{y\ TEST}$ = 521 MPa) with transverse reinforcement consisting of #3 or #4 grade 40 bars ($f_{y\ TEST}$ = 394 MPa). CFRP sheets with a total thickness of 0.22 mm were epoxyed to the column surface with fibers oriented perpendicular to the longitudinal axis of the retrofitted columns. The mechanical properties of the CFRP sheets are listed in Table 2.

3 Quasi-static tests and results

The specimens were subjected to predetermined displacement excursions during which the lateral load was applied on the top of the frames in a reversed cyclic pattern. The deformation at the end of each cycle was progressively increased from a displacement corresponding to a drift ratio of 0.125% in the first cycle to 2.0%, 3.0%, or 6.0%, at the end of the tests. The force-deformation curves for these specimens are given in Fig. 3. Details of the experiment and test results can be found in the preliminary report (Huang *et al*., 2006).

4 Pushover analysis and results

As mentioned earlier, in performance-based seismic design, the structural behavior of a building has to be evaluated at various levels of deformation. Since it is not practical to conduct a nonlinear structural test on every structure, engineers must rely on available documents and analytical tools to evaluate the force-displacement relationship of a structure. To see how current literature

Table 2 Mechanical properties of CFRP sheets

Modulus of elasticity	Ultimate strain	Allowable stress	Adhesive strength
230,535 MPa	0.021	3,458 MPa	1.96 MPa

applies to the above units, a pushover analysis was performed based on some of the prevailing industrial guidelines. In this analysis, the mechanical behaviors of individual frame components were represented by the generalized load-deformation model proposed by ATC-40, as shown in Fig. 4. In this model, the linear response of a structural component is depicted by the straight line between points *A* (unloaded situation) and *B* (the effective yield point). As deformation progresses, the component gets little or no increase in resistance until Point *C*, after which a significant strength degradation (line *CD*) takes place. Beyond point *D*, the component

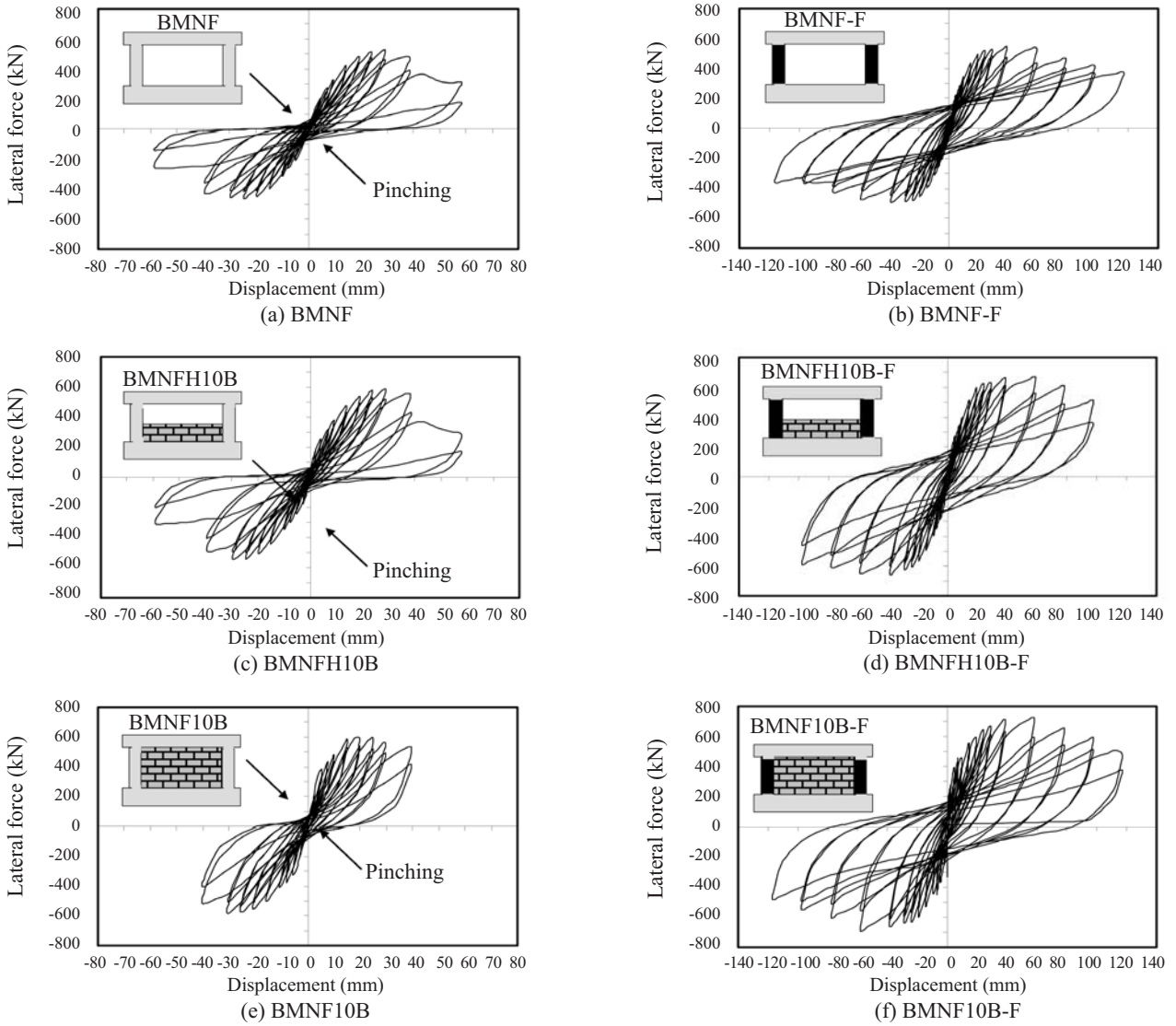

Fig. 3 Force-deformation curves of tested units

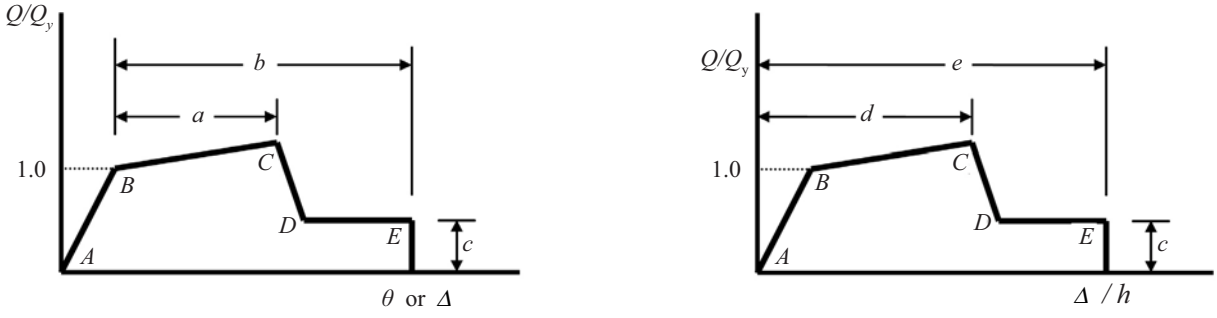

Fig. 4 Generalized force-deformation relations for concrete elements (ATC-40, 1996)

responds with substantially reduced strength up to point *E*, and essentially no strength afterwards. In Fig. 4(a), the deformation of a component is expressed in terms of either strain, curvature, rotation, or elongation. The parameters *a* and *b* refer to the portions of deformation that occur after yield, and the parameter *c* is the residual resistance of the element after the sudden reduction from point *C* to *D*. In Fig. 4(b), the component deformations are expressed in terms of shear angle or tangential drift ratio with parameters *d* and *e* referring to the total deformations measured form the origin. In both Figs. 4(a) and 4(b), the strength of the component is expressed in terms of the normalized forced (Q/Q_{CE}). Recommendations on the values of the parameters used in the above model, i.e., values of *a*, *b*, *c*, *d*, and *e*, can be found in FEMA 356 for various types of structural components.

In this analysis, the elastic stiffnesses of beams and columns in the tested frames were calculated based on the recommendations of FEMA 356 (see Table 3). Since no external vertical load was applied on specimens, the compression force due to gravity load in any frame column was well under $0.3A_g f'_c$. Therefore, flexural and shear rigidities of $0.5E_cI_g$ and $0.4E_cA_g$ were applied to all beams and columns, respectively. For masonry infills, the force-deformation relationship is relatively complicated (Bertero and Brokken, 1983; Mehrabi *et al*., 1996), and the compression strut model (see Fig. 5) recommended by FEMA 356 was used for the calculation of strengths and effective stiffnesses of the panels.

The assignment of hinges in the computer models was determined based on the strengths of individual components and mechanisms which were most likely to occur in each frame. For example, only flexural hinges were assigned in the columns of frames jacketed by CFRP sheets, i.e., units BMNF-F, BMNFH10B-F, and BMNF10B-F, since shear failure did not occur in these members due to the strength enhancement by CFRP. For other units, i.e., BMNF, BMNFH10B, and BMNF10B, an extra shear hinge was added at the mid-height of each column considering the unreliable shear capacity provided by inadequate transverse reinforcement. And for the masonry infills, a one-way axial compression hinge was assigned at the midpoint of each equivalent compression strut.

The axial and flexural strengths of a concrete column can be defined by the interaction diagram of the column. In this study, the flexural strength of a column was taken at the intersection of the curve, which represented the moment and axial force development in the critical sections of the column; and the interaction diagram, which was calculated based on actual material strengths, as shown in Fig. 6. With the flexural strengths at both ends of the columns calculated, the hinge parameters of these columns were found in FEMA 356 (see Table 3, Table 4, and Fig. 4), and the pushover curve for unit BMNF-F was obtained accordingly, as shown in Fig. 7. For illustration purposes, the actual force-deformation curve of the frame was obtained by averaging the envelope curves of its hysteresis loops in both directions of deformation, as shown in Fig. 3(b), and exhibited in the same figure. The relationships between the load and inelastic deformation of hinges obtained based on FEMA 356 provisions were also presented, as given in Fig. 8, and compared to the experimental results. It can be seen that the calculated column flexural strengths were fairly close to the tested values with the maximum errors less than 7%. Bearing in mind that the interaction diagram theory was originally developed for monotonically loaded elements, the differences between the calculated and actual strengths of the columns are incredibly small for cyclic loaded members. As for the deformability of columns, the deformation at which clear strength degradation occurred was slightly greater than predicted; and for the stiffness of the columns, it is apparent that the effective flexural stiffness of columns specified by FEMA 356, $0.5E_cI_g$, resulted in a higher rigidity than the actual rigidity of the frame.

For unreinforced masonry panels, FEMA 356 provides the following equation for the calculation of the expected masonry shear strength, v_{me}:

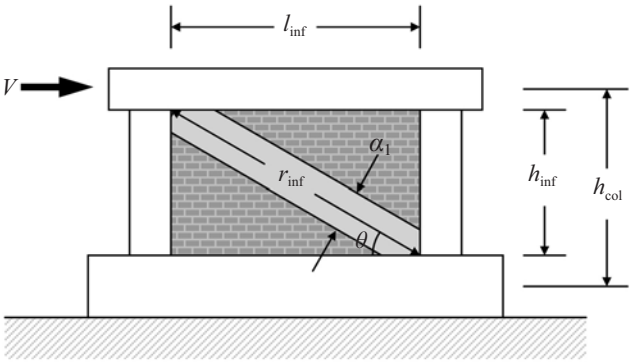

Fig. 5 Compression strut analogy (FEMA, 2000)

Table 3 Effective stiffness values (FEMA, 2000)

Component	Flexural rigidity	Shear rigidity
Beams (nonprestressed)	$0.5E_cI_g$	$0.4E_cA_w$
Columns with compression due to design gravity loads $\geq 0.5A_g f'_c$	$0.7E_cI_g$	$0.4E_cA_w$
Columns with compression due to design gravity loads $\leq 0.3\ A_g f'_c$ or with tension	$0.5E_cI_g$	$0.4E_cA_w$

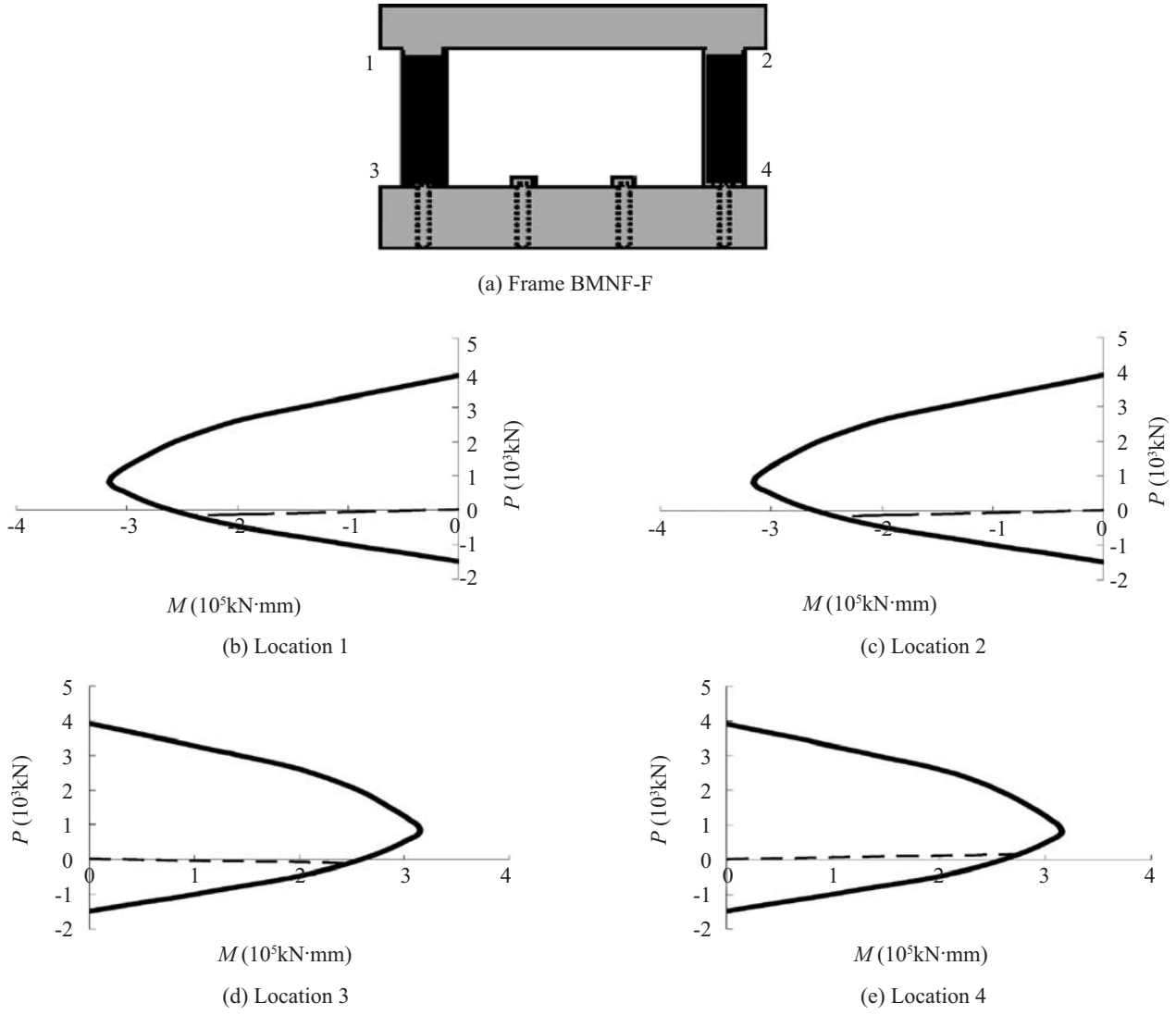

(a) Frame BMNF-F

(b) Location 1

(c) Location 2

(d) Location 3

(e) Location 4

Fig. 6 Determination of column flexural strengths (Frame BMNF-F)

Table 4 Modeling parameters for frame components (FEMA, 2000)

Conditions		Modeling parameters*					Units applicable
		a	*b*	*c*	*d* **	*e*	
Beams		0.025	0.05	0.2	n.a.	n.a.	All
Columns	Flexure	0.02	0.03	0.2	n.a.	n.a.	All
	Shear	n.a.	n.a.	n.a.	0	0	BMNF, BMNFH10B, BMNF10B
Infill Panels		n.a.	n.a.	n.a.	0.011	n.a.	BMNF10B, BMNF10B-F

Note: * See Fig. 4 for the definitions of *a*, *b*, *c*, *d*, and *e*.

** The value of *d* for infill panels were obtained from interpolation of FEMA recommended values

$$v_{me} = \frac{0.75\left(0.75v_{te} + \frac{P_{CE}}{A_n}\right)}{1.5} \quad (1)$$

in which P_{CE} is the expected gravity compressive force applied to the wall, A_n is the area of net mortared/grouted section of the wall, and v_{te} is the average bed joint shear strength determined from bed joint shear test. Since no bed joint test was conducted in this experiment, the shear strength of the infills was taken as the lower-bound value of 0.186 MPa (for masonry with $f'_m = 6.2$ MPa) multiplied by a factor of 1.3, as specified by FEMA 356, which gave an expected shear strength of 0.242 MPa for the masonry panels in both BMNF10B and BMNF10B-F. FEMA also gives the following equation for the calculation of the width of the equivalent diagonal compression strut that represents the in-plane stiffness of a solid unreinforced

masonry infill panel before cracking:

$$a_1 = 0.175\ (\lambda_1 h_{col})^{-0.4} r_{inf} \quad (2)$$

where

$$\lambda_1 = \left[\frac{E_{me} t \sin 2\theta}{4 E_c I_c h_{inf}}\right]^{\frac{1}{4}} \quad (3)$$

is the coefficient used to determine equivalent width of infill strut, r_{inf} is the diagonal length of the infill panel, h_{col} is the column height between centerlines of beams, h_{inf} is the height of the infill panel, $E_c I_c$ is the expected flexural rigidity of the columns, E_{me} is the expected modulus of elasticity of infill material, t is the thickness of the infill panel and equivalent strut, and θ is the angle between the diagonal of the panel and the horizontal plane. The definitions of h_{col}, h_{inf}, a_1, θ, and r_{inf} are also illustrated in Fig. 5. The story drift representing the nonlinear deformability of the masonry infills, d (see Fig. 4(b)), was taken as 1.1% through interpolation based on values provided in FEMA 356 (see Table 4).

For simplicity, the strength contributions of masonry infills in the specimens were obtained by subtracting the load-deformation curves of pure frame units (BMNF and BMNF-F) from infilled frames with similar frame strengths (BMNF10B and BMNF10B-F). Figure 9 shows the averaged load-deformation curve of the infill panels obtained from the test for units BMNF10B and BMNF10B-F and the curve obtained based on FEMA 356. It appears that the actual behavior of the masonry infills significantly differed from the behavior predicted by the FEMA model, possibly caused by the frame-panel interaction. Nevertheless, the FEMA model did produce a good estimation of both the panel stiffness before cracking and the shear strength at the ultimate stage. The force-deformation curves of unit BMNF10B-F obtained based on FEMA 356 and the test are shown in Fig. 10. It is seen that the FEMA model underestimated the ultimate shear strength of the jacketed masonry infilled concrete frame BMNF10B-F, which could possibly have resulted from neglecting the beneficial confining effect of the CFRP sheet jacketing.

For partially confined (or perforated) infills, a complete load-deformation model was proposed by Chen. In this model, the load-deformation curve of a clay brick infill confined on both sides and bottom of the panel, as in units BMNFH10B and BMNFH10B-F, was divided into three stages based on the amount of

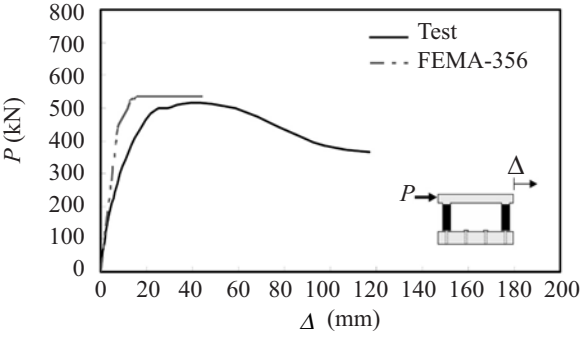

Fig. 7 Force-deformation relations of unit BMNF-F

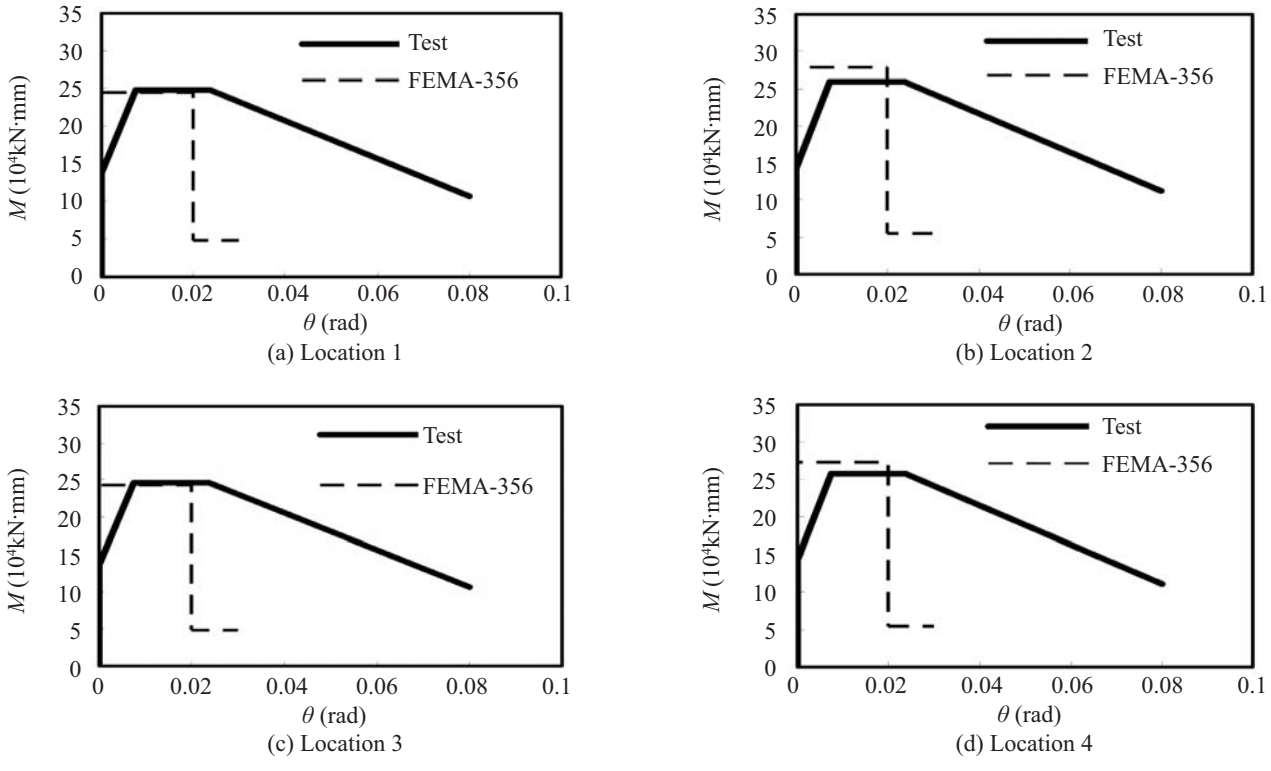

Fig. 8 Load vs. inelastic deformation for column flexural hinges in frame BMNF-F at different hinge locations shown in Fig. 6(a)

deformation (see Fig. 11). In the first (ascending) stage ($\Delta < \Delta_u$), the curve is defined by a cubic equation:

$$V = \left[3\left(\frac{\Delta}{\Delta_u}\right) - 3\left(\frac{\Delta}{\Delta_u}\right)^2 + \left(\frac{\Delta}{\Delta_u}\right)^3 \right] V_n \tag{4}$$

In the second (descending) stage ($\Delta_u \le \Delta \le 2\Delta_u$), the curve is represented by the following relationship:

$$V = V_n - (\Delta - \Delta_u)\frac{V_n - V_r}{\Delta_u} \tag{5}$$

And after sliding occurs ($\Delta > 2\Delta_u$), the residual strength remains constant:

$$V = V_r \tag{6}$$

To calculate the lateral strength of the infill, V_n, Chen proposed the following equation according to the experimental results of Chang (1997) and Kang (1996):

$$V_n = (0.7\tau_f + 0.113 f_{mbt})\, l_{inf}\, t \tag{7}$$

where

$$\tau_f = 0.0258 f_{mc}^{0.885} \tag{8}$$

is the friction stress along the bed joints,

$$f_{mbt} = 0.232 f_{mc}^{0.338} \tag{9}$$

is the tensile strength of the brick-mortar interface, and f_{mc} is the compressive strength of the mortar. In this analysis, the lateral strength of the 85 cm (half of the clear column height) high brick panel was calculated as 59.7 kN by substituting the measured mortar strength (4.3 MPa) into Eqs. (7), (8), and (9). The displacement at which the panel reaches its maximum strength, Δ_u, is calculated as

$$\Delta_u = \left[1.475\frac{l_{inf}}{h_{inf}} + 2.263\frac{h_{inf}}{l_{inf}} + 2.225\left(\frac{h_{inf}}{l_{inf}}\right)^3 \right] \frac{V_n}{E_u t} \tag{10}$$

where E_u, the secant modulus of elasticity at $\Delta = \Delta_u$, can be obtained from the following equation

$$E_u = 22.5\left(1.67 - 0.64\frac{h_m}{l_m}\right) f_{bc}^{0.7} f_{mc}^{0.3} \tag{11}$$

in which f_{bc} is the compressive strength of the clay brick unit (measured 20.0 MPa in average for tested units). The residual strength, V_r, of the panel is given by Chen as

$$V_r = 0.7\tau_f\, t\, l_{inf} \tag{12}$$

or $0.6V_n$, whichever is less. It should be noted that the deformation Δ in these equations was taken as the lateral displacement at the top of the panel, i.e., at the mid-height of frames. Figure 12 shows the relationship between the average contribution of the masonry infills in frame strength for units BMNFH10B and BMNFH10B-F and the frame deformation at the top of the frame, obtained from both the test results and Chen's model. It can be found that the contribution of the infill calculated from Chen's model was much lower than the tested value. However, since the displacements at the top of the panels were not measured during the test, the above discrepancy could have come from the nonlinear response of the free column sections as well as the frame-panel interaction. The force-deformation curves of unit BMNFH10B-F obtained from both Chen's model and the test results are shown in Fig. 13.

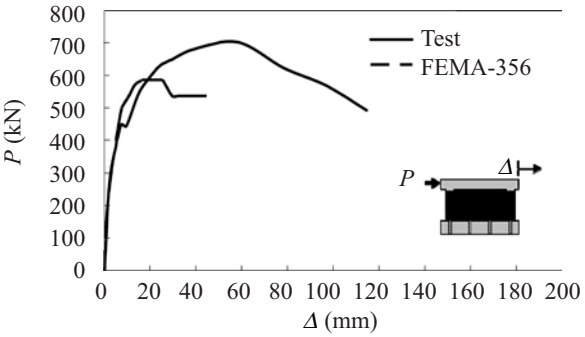

Fig. 10 Force-deformation curves of unit BMNF10B-F

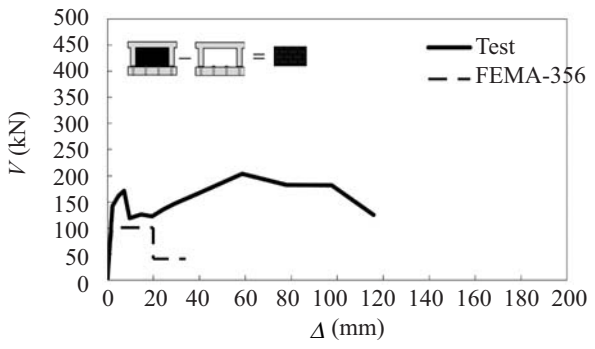

Fig. 9 Averaged strength contribution of the infills in units BMNF10B and BMNF10B-F

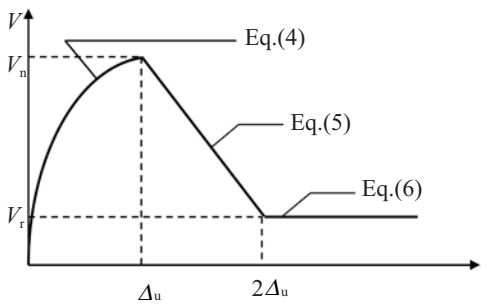

Fig. 11 Load-deformation relation of a partially confined brick infill

The shear strength of concrete columns can be calculated from the following equation per ACI 318

$$V_n = V_c + V_s \tag{13}$$

where V_c and V_s are the strengths provided by concrete and steel reinforcement, respectively (see Table 5). For columns whose failure was controlled by shear, FEMA 356 suggests that the deformation of such members should be kept in the elastic range due to the brittle nature of the mechanism. In other words, the strength of the column should be considered totally lost once the shear force in the column reaches its shear capacity. Table 6 shows the shear strengths of the columns and frames in units BMNF, BMNFH10B, and BMNF10B, calculated using actual material strengths. Comparisons between force-deformation curves of these frames based on the ACI-FEMA provisions and test results are given in Figs. 14 through 16. It is shown that for all three

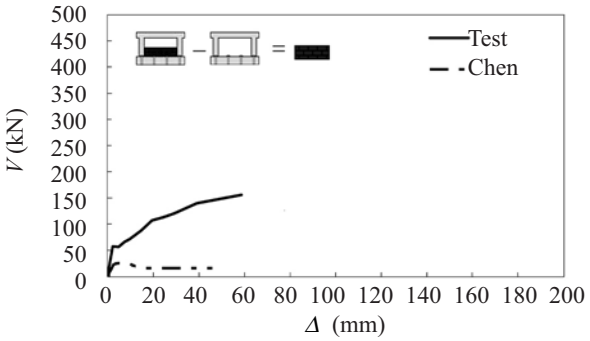

Fig. 12 Averaged strength contribution of the infills in units BMNFH10B and BMNFH10B-F

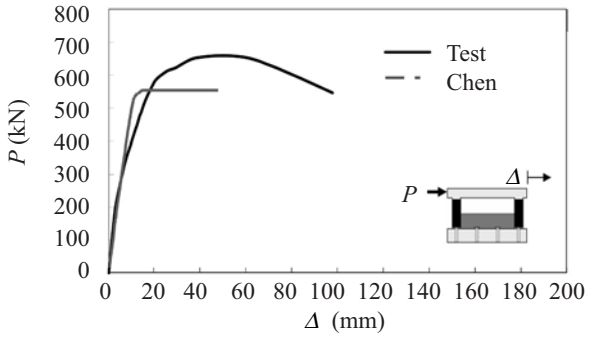

Fig. 13 Force-deformation curves of unit BMNFH10B-F

Table 5 Shear strengths of members provided by concrete and steel (ACI-318, 1999)

V_c			V_s
$N_u > 0$	$N_u = 0$	$N_u < 0$	
$\left(1+\frac{N_u}{14A_g}\right)\left(\frac{\sqrt{f'_c}}{6}\right)b_w d$	$\left(\frac{\sqrt{f'_c}}{6}\right)b_w d$	$\left(1+\frac{0.3N_u}{A_g}\right)\left(\frac{\sqrt{f'_c}}{6}\right)b_w d$	$\frac{A_v f_y d}{s} \le \frac{2\sqrt{f'_c}b_w d}{3}$

Table 6 Shear strengths of frames in units BMNF, BMNFH10B, and BMNF10B calculated based on ACI 318

Frame ID		N_u	V_c	V_s	$V_{n\,col}$	$V_{n\,frame}$
BMNF	L	-65	86	81	167	350
	R	93	102		183	
BMNFH10B	L	-59	86	81	167	349
	R	84	101		182	
BMNF10B	L	-115	76	81	157	341
	R	108	103		184	

Note: Unit = kN

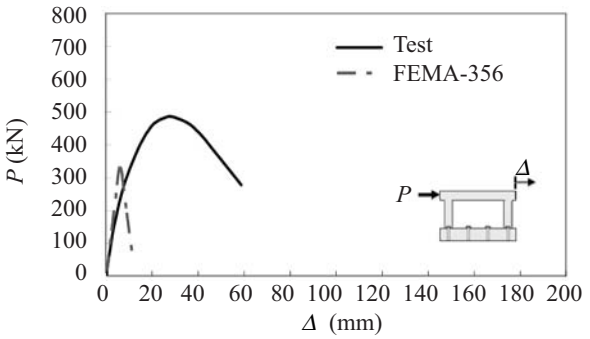

Fig. 14 Force-deformation curves of unit BMNF

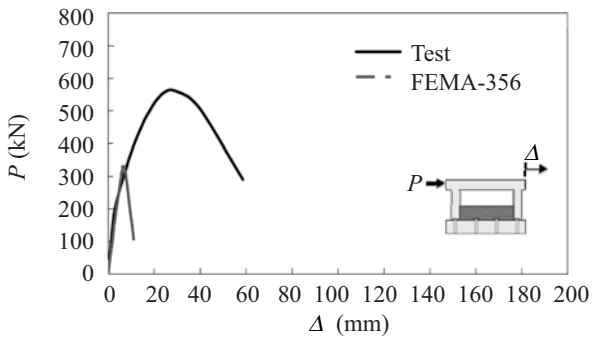

Fig. 15 Force-deformation curves of unit BMNFH10B

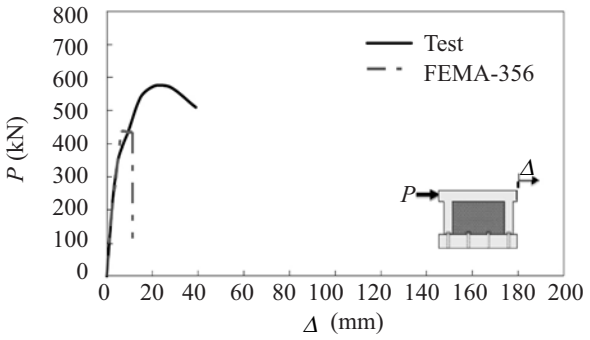

Fig. 16 Force-deformation curves of unit BMNF10B

frames, the measured shear strengths are significantly higher than the code values. It should be recognized that for the calculation of the column shear strength, ACI 318 assumes a 45-degree failure surface and considers only the transverse reinforcement intersected by this surface contributive to the shear strength of the member. Nevertheless, the shear failure in these columns developed in a plane oriented at a greater angle (from the direction of the shear) and therefore involved more transverse reinforcement in the mechanism (Huang *et al*., 2006). A higher shear strength might have developed accordingly.

5 Conclusions

A nonlinear pushover analysis was performed for six reinforced concrete frames with full, partial or without masonry infills. The load-deformation relationships of individual components, such as concrete columns and masonry infill panels, were established based on ACI 318, FEMA 356, and Chen's model. The structural behavior obtained from the analysis and test results was compared on both component and frame levels for each specimen. It was found that for bare frames, the flexural strengths of columns calculated from interaction diagrams were very close to the actual strengths obtained from the test results, with no errors greater than 7%. Since the strengths based on ACI 318 indicated a slight overestimation in two of the four hinge strengths, it is suggested that a reduction factor should be used for the calculation of column strengths in a pushover analysis. Furthermore, in order to account for the strength degradation of columns after yield, the strength increase due to strain hardening should not be considered.

With the flexural behavior of columns identified, FEMA 356 and Chen's models were incorporated in the analysis of fully and partially confined infills, respectively. For fully confined infills, the equivalent strut model specified in FEMA 356 was able to give a reasonable prediction on both uncracked stiffness and lateral strength of the masonry panels; for partially confined infills, on the other hand, Chen's model seemed to be conservative in estimating the strength contribution of the infills to the frames. On deformability, both models were able to prescribe a deformation level at which the lateral strength of the infills could be reliably sustained. However, due to the dispersion of the constitutive relationships between different infill configurations, further investigation should be considered.

For columns that failed in shear, the combination of ACI and FEMA specifications was found conservative in predicting the shear resistance of the columns. However, during a real earthquake, the lateral load acting in another (perpendicular) direction is likely to generate additional cracks in the columns and lower the shear strengths.Under this circumstance, the ACI-FEMA provisions would supply a safety margin and therefore should be considered appropriate for design considerations.

In the present study, flexural hinges in the columns of frames jacketed by CFRP sheets were assigned to account for the strength enhancement by CFRP. However, these would not be enough for a more reasonable incorporation of the confinement effect of the CFRP sheets. It should also be noted that a more satisfactory modeling of the effect of both the partial or full masonry infills and the CFRP jacketing would require that more reliable test results be provided.

Acknowledgements

This study was sponsored by the Science Council of Chinese Taipei (Grant No. SC-92-2625-Z-027-003) while both the facility and the specimens were provided by the Center for Research on Earthquake Engineering in Taipei. The contributions of the above organizations to this research were gratefully acknowledged.

References

ACI Committee 318 (1999), *Building Code Requirements for Reinforced Concrete and Commentary*. *ACI 318M-99* and *ACI 318R-99*, American Concrete Institute, Detroit, Michigan.

Allahabadi R and Powell GH (1988), *DRAIN-2DX User Guide*. *Report No. UCB/EERC-88/06*, Earthquake Engineering Research Center, University of California, Berkeley.

ATC-40 (1996), *Seismic Evaluation and Retrofit of Concrete Buildings*, *Report No. ATC-40*, Prepared by the Applied Technology Council for the California Seismic Safety Commission. Redwood City, California.

Bertero VV and Bokken S (1983), "Infills in Seismic Resistant Buildings," *Journal of Structural Engineering*, ASCE, **109**(6): 1337-1361.

Chang WD (1997), "Seismic Test, Analysis, and Application of RC Frames with Infilled Brick Walls," *PHD Thesis*, Department of Architecture, National Cheng Kung University.

Chung YS, Meyer C and Shinozuka M (1988), "SARCF User Guide: Seismic Snslysis of Teinforced Concrete

Frames," *Technical Report NCEER-88-0044*, State University of New York at Buffalo.

FEMA (1997), "NEHRP Guidelines for the Seismic Rehabilitation of Buildings," *FEMA 273*, Prepared by the Applied Technology Council for the Building Seismic Safety Council, Washington, D.C.

FEMA (2000), "Prestandard and Commentary for the Seismic Rehabilitation of Buildings," *FEMA 356*, Prepared by American Society of Civil Engineers for Federal Emergency Management Agency, Washington, D.C.

Giberson MF (1967), "The Response of Nonlinear Multistory Structures to Earthquake Excitation," Earthquake Engineering Research Laboratory, California Institute of Technology, Pasadena, California.

Habibullah A (1995), ETABS v6.0: *Three Dimensional Analysis of Building Systems*, User's manual, Computers and Structures, Inc., Berkeley, California.

Huang CH, Sung YC and Tsai CH (2006), "Experimental Study and Modeling of Masonry-infilled Concrete Frames with and Without CFRP Jacketing," *Structural Engineering and Mechanics*, **22**(4): 449-467.

Kanaan AE and Powell GH (1973), "DRAIN-2D: A General Purpose Computer Program for Dynamic Analysis of Inelastic Plane Structures," *Report No. UCB/EERC-73/06 and 73/22*, Earthquake Engineering Research Center, University of California, Berkeley.

Kang CR (1996), "Test and Analysis of RC Frames Retrofitted After Earthquake — by Jacketing Method," *Maser's thesis*, Department of Architecture, National Cheng Kung University.

Mehrabi AB, Shing PB, Schuller MP and Noland JL (1996), "Experimental Evaluation of Masonry-infilled RC Frames," *Journal of Structural Engineering*, ASCE, **122**(3): 228-237.

Otani S and Sozen MA (1972), "Behavior of Multistory Reinforced Concrete Frames During Earthquakes," *Civil Engineering Studies*, *Structural Research Series No. 392*, University of Illinois, Urbana.

Oughourlian CV and Powell GH (1982), "ANSR-III: General Purpose Computer Program for Nonlinear Structural Analysis," *Report No. UCB/EERC-82/21*, Earthquake Engineering Research Center, University of California at Berkeley.

Park YJ, Reinhorn AM and Kunnah SK (1987), "IDARC: Inelastic Damage Analysis of Reinforced Concrete Frame – shear Wall Structures," *Technical Report NCEER-87-0008*, State University of New York at Buffalo.

Paulay T and Priestley MJN (1992), *Seismic Design of Reinforced Concrete and Masonry Buildings*, John Wiley & Sons, New York, USA.

Saiidi M and Sozen MA (1979), "Simple and Complex Models for Nonlinear Seismic Response of Reinforced Concrete Structures," *Civil Engineering Studies*, *Structural Research Series No. 392*, University of Illinois, Urbana.

SEAOC (1995), Vision 2000 Progress Report. *Proceedings of 1995 Convention*, Structural Engineers Association of California, San Francisco, California.

Takeda T, Sozen MA and Nielsen NN (1970), "Reinforced Concrete Response to Simulated Earthquake," *Journal of Structural Division*, American Society of Civil Engineers, **96**(12): 2557-2573.

Tsai KC, Hsiao CP and Bruneau M (2000), "Overview of Building Damages in 921 Chi-Chi Earthquake," *Earthquake Engineering and Engineering Seismology*, Chinese Taiwan Society for Earthquake Engineering**,** **2**(1): 93-118.

Wilson EL (1995), "SADSAP v2.04: Static and Dynamic Structural Analysis Programs," *Structural Analysis Programs*, Inc., El Cerrito, California.